Vol 18 No 11, November 2009
1674-1056/2009/18(11)/4981-07

Chinese Physics B

© 2009 Chin. Phys. Soc.
and IOP Publishing Ltd

Electronic, thermodynamic and elastic properties of pyrite RuO_2*

Yang Ze-Jin(杨则金)[a], Guo Yun-Dong(郭云东)[b], Wang Guang-Chang(王光昶)[c], Li Jin(李 劲)[a,d], Dai Wei(戴 伟)[a,e], Liu Jin-Chao(刘锦超)[a]†
Cheng Xin-Lu(程新路)[a], and Yang Xiang-Dong(杨向东)[a]

[a] *Institute of Atomic and Molecular Physics of Sichuan University, Chengdu* 610065, *China*
[b] *School of Physics and Electronic Information Engineering, Neijiang Normal University, Neijiang* 641112, *China*
[c] *Teaching and Researching Section of Physics, Chengdu Medical College, Chengdu* 610083, *China*
[d] *College of Material and Chemical Engineering, Hainan University, Haikou* 570228, *China*
[e] *Chinese Academy of Engineering Physics, Mianyang* 621900, *China*

(Received 31 October 2008; revised manuscript received 27 February 2009)

This paper calculates the elastic, thermodynamic and electronic properties of pyrite ($Pa\bar{3}$) RuO_2 by the plane-wave pseudopotential density functional theory (DFT) method. The lattice parameters, normalized elastic constants, Cauchy pressure, brittle–ductile relations, heat capacity and Debye temperature are successfully obtained. The Murnaghan equation of state shows that pyrite RuO_2 is a potential superhard material. Internal coordinate parameter increases with pressure, which disagrees with experimental data. An analysis based on electronic structure and the pseudogap reveals that the bonding nature in RuO_2 is a combination of covalent, ionic and metallic bonding. A study of the elastic properties indicates that the pyrite phase is isotropic under usual conditions. The relationship between brittleness and ductility shows that pyrite RuO_2 behaves in a ductile matter at zero pressure and the degree of ductility increases with pressure.

Keywords: elastic property, thermodynamic property, electronic structure
PACC: 6220D, 6540, 7115H

1. Introduction

RuO_2 has been studied extensively owing to its interesting fundamental properties[1−7] and potential superhard characteristics.[2,3] An extensive search for new superhard materials has been undertaken during recent years,[8] and a possible new class of hard materials has been suggested: the transition-metal dioxides containing heavy elements;[9] typically, the bulk modulus of modified fluorite RuO_2 was found to be 399 GPa,[10] which was the highest value reported in a material, except for diamond with a value of 442 GPa.[11]

Under ambient pressure, many MX_2 compounds take on either the rutile or the $CaCl_2$ structure;[12] the primary difference between these two structures involves a rotation about the c axis of the MX_6 octahedra. Under usual conditions, RuO_2 has a rutile structure,[10] and it transforms to a $CaCl_2$ structure at about 6 GPa[13] or 11.8 GPa,[14] and then to a modified fluorite structure at about 12 GPa, the $Pa\bar{3}$ structure can transform to a $Fm\bar{3}m$ at about 89 GPa or 97 GPa.[3]

The electronic structure and elastic properties have also been the subject of considerable attention, and a detailed study of electronic structure has been reported by Glassford and Chelikowsky.[15] A full-potential linear muffin-tin orbital calculation on the electronic structure of fluorite RuO_2 has been performed by Lundin *et al.*[16] Elastic properties focused on the $Pa\bar{3}$ phase have been investigated by Tse *et al.*[3] The band structure, density of states and charge density of the rutile and $CaCl_2$ phases have been researched by Benyahia *et al.*[17] The Fermi surface of rutile RuO_2 has been studied by Yavorsky *et al.*[18] First-principles electronic-structure calculations have been studied by Glassford and Chelikoowsky.[19] The electronic, optical properties and stabilization of rutile RuO_2[2,15,20,21] have been described by density functional theory (DFT). Hardness and elasticity[22] of RuO_2 and Raman scattering observation of the rutile-$CaCl_2$ phase transition have been probed experimentally. Scanning tunnelling microscope growth of RuO_2 has been reported by Zhang *et al.*[23]

*Project supported by the China Scholarship Council (CSC) and the National Natural Science Foundation of China (Grant Nos 10676025 and 10574096).
†Corresponding author. E-mail: jliu@scu.edu.cn

2. Theoretical methods

In the present study, we elaborate on the elastic, thermodynamic properties and electronic structure of pyrite RuO_2 under high pressures via first-principles. Our calculations were performed using the plane-wave pseudopotential DFT method by the CASTEP.[24,25] In the electronic structure calculations, we used the non-local ultrasoft pseudopotential introduced by Vanderbilt,[26] together with the revised Perdew–Burke–Ernzerhof (RPBE) of the generalized gradient approximation (GGA) exchange-correlation function.[27,28] A plane wave basis set with energy cutoff 600.0 eV[3] has been applied. Pseudo atomic calculations have been performed for Ru $4s^2$ $4p^6$ $4d^7$ $5s^1$ and O $2s^2$ $2p^4$. For the Brillouin-zone sampling, the 12×12×12 Monkhorst–Pack mesh[29] has been adopted, where the self-consistent convergence of the total energy was at 5.0×10^{-7} eV/atom.

3. Results and discussion

The obtained Murnaghan equations of state (EOS)[30] under ambient conditions are listed in Table 1, together with the experimental data[31] and theoretical results.[3,32] It is found that they agree well. Comparing the volume compressibility with the ultrastiff cubic TiO_2[33] at 100 GPa, the obtained compressibility is nearly identical (79.88%). The obtained bulk modulus is slightly smaller than that of the TiO_2 with a value of 282/395 GPa. Therefore, the definition of RuO_2 as a potential ultrahard material seems highly plausible.[3] Transition metal oxides, such as OsO_2, are usually superhard, especially their carbides and nitrides, with a bulk modulus of 302 GPa. Zheng[34] indicated that OsC is a promising superhard material with a bulk modulus of 396 GPa, which is higher than that of c-BN (369 GPa)[35] and is lower than that of diamond (444 GPa /443 GPa).[36−40] At 100 GPa, the obtained pyrite RuO_2 compressibility is comparable to that of superhard materials, such as diamond (85%), c-BN (83%), OsO_2 (80%) and OsC (84%), respectively. Meanwhile, the internal structure parameters of the oxygen atom are calculated; the obtained fractional coordinate increases with pressure, which coincides with the case of the calculated results.[3] Surprisingly, experimental results[31] decrease with pressure.

Table 1. The calculated lattice constants, aggregate elastic modulus, pressure derivatives of bulk modulus and the elastic constants for pyrite RuO_2 at $P = 0$ and $T = 0$. (LDA represents the localized density approximation.)

method	a/Å	B_0/GPa	B_0'/GPa	u/Å	c_{11}/GPa	c_{44}/GPa	c_{12}/GPa
GGA	4.9018	273.47	3.98	0.3497	430	148	162
LDA	4.7756	368.38	3.41	0.3508	541	169	243
Exp[31]	4.85892	399	3.5	0.3511			
Ref.[3](GGA)	4.884	299/334	3.9	0.3503	450	189	147
Ref.[3](LDA)	4.792	346/380	4.2	0.3525			
Ref.[32]	5.00	386	2.75		383	133	144

According to the elastic constants, we can obtain all of the other thermodynamic quantities of a solid, and these elastic coefficients obey a generalized elastic stability criterion[38−40] for cubic crystals under hydrostatic pressure, $c_{11} - c_{12} > 0$, $c_{11} + 2c_{12} > 0$, $c_{44} > 0$. Analysis indicates that the pyrite structure is elastically stable up to 150 GPa.

The deviation from the Cauchy relation $\delta = c_{12} - c_{44} - 2P$ is a measure of the contribution from the noncentral many-body force since the Cauchy relation $c_{12} = c_{44} + 2P$ should be satisfied when interatomic potentials are purely central. Figure 1 shows the pressure dependence of δ. For pyrite structure, the deviation δ becomes larger as the pressure increases, which proves that the noncentral many-body force becomes more and more important at high pressures. Thus, it is necessary to consider third-order and fourth-order elastic constants when we discuss the anharmonic properties by means of elastic constants at high pressures. For the fluorite structure, the devia-

tion δ becomes larger as the pressure increases up to about 20 GPa, then the deviation δ becomes smaller as pressure increases; the deviation δ approaches zero when pressure increases up to about 115 GPa, and all of the Cauchy pressures are negative. The Cauchy pressure will be positive when the pressure is larger than 115 GPa. Therefore, one can easily conclude that the noncentral contribution of the fluorite structure is more complicated than that of the pyrite structure. The fluorite structure shows more harmonicity of the vibrational states or linearity of the atomic force field resulting from the ion-overlapping and covalent bonding[41] under special conditions; the large deviation implies the existence of a large component of anharmonic forces between atoms, resulting somewhat from covalence or charge transfer between ions.

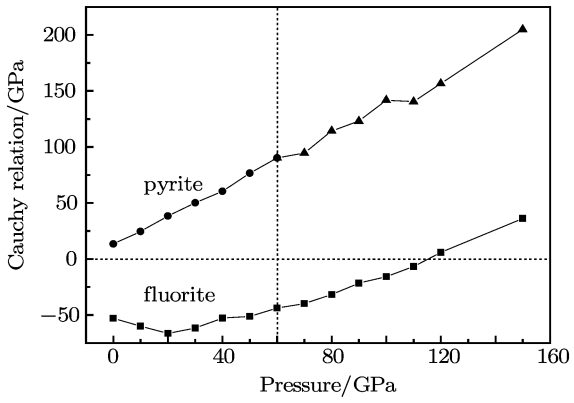


Fig.1. Pressure dependence of Cauchy relation.

The Zerner[42−45] elastic anisotropic parameter A, which is the ratio of two shear moduli c_{44} and $(c_{11} - c_{12})/2$, becomes unity for isotropic elasticity. It is known that even the cubic crystal, which has an isotropic structure, also has elastic anisotropy as a result of a fourth rank tensor property of elasticity. According to the obtained elastic constants, we can know that the pyrite phase RuO_2 exhibits low elastic anisotropy at zero pressure and the degree of the anisotropy increases with pressure; the calculated results are 1.06 at 0 GPa and 1.23 at 150 GPa.

In order to investigate the elasticity of RuO_2 in more detail, we have used normalized elastic constants c'_{ij}.[44,45] The value of c'_{ij} is obtained by dividing a specific elastic constant with the bulk modulus

$$c'_{ij} = c_{ij}/B = 3c_{ij}/(c_{11} + 2c_{12}). \quad (1)$$

Divided by the bulk modulus, the interatomic forces are normalized with an average restoring force of the system. At zero pressure, if a cubic crystal is elastically ideal, namely the isotropic Cauchy solids, 1.8, 0.6 and 0.6 for c'_{11}, c'_{12} and c'_{44} are found, respectively. Analysis found that our calculated results are in good agreement with the above values at ambient conditions: each is 1.71, 0.64 and 0.59. These coincidences are also confirmed by the anisotropic parameter A. We extended the concept of the normalized elastic constant to the high-pressure condition. The c'_{ij} of RuO_2 as a function of pressure is plotted in Fig.2. It is found that all normalized elastic constants of c'_{ij}, c'_{11} and c'_{44} slowly decrease with increasing pressure. Comparing c'_{11} with the decrease of 29%, c'_{44} rapidly decreases to the magnitude of 52%. The value of c'_{12} slowly increases and the increase is almost linear. Compared with c'_{11} and c'_{44} under pressure, c'_{12} has a moderate increase with a value of 39%, which means that they are all quite sensitive to pressure.

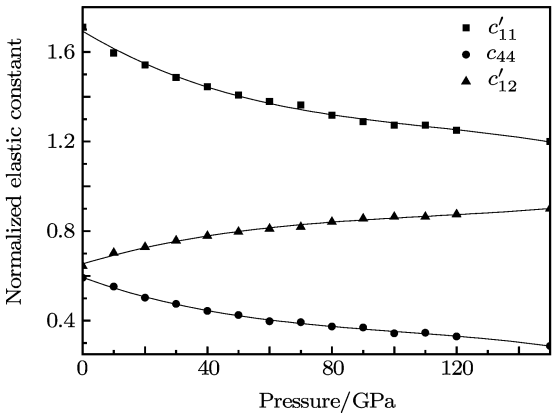


Fig.2. Normalized elastic constant variation with pressure.

The value of the Poisson ratio for covalent materials is small ($\sigma = 0.1$), whereas for ionic materials a typical value of σ is 0.25.[46] The obtained Poisson ratio (0.2546), being much higher than the covalent limit (≈ 0.20),[47] suggests strong ionicity or a weak covalent component. In our cases, the values of σ for RuO_2 varies from about 0.2546 to 0.3946, i.e., a higher ionic contribution in intra-atomic bonding for RuO_2 should be assumed at ambient conditions, and the increase implies that most of the bonds are ionic.

For covalent and ionic materials, the typical relations between the bulk and shear modulus are $G \approx 1.1B$ and $G \approx 0.6B$, respectively. For pyrite RuO_2, the Voigt–Reuss–Hill (VRH) estimations[48−50] of G_{VRH}/B_{VRH} are 0.5679 at 0 GPa and 0.2321 at 150 GPa, indicating that ionic bonding and ductility matter are more suitable at zero pressure and the

degree of ductility rises at high pressures. For evaluating material brittleness Pugh[51] introduced the $B_{\rm VRH}/G_{\rm VRH}$ ratio: the material is brittle if the ratio is less than the critical value 1.75. Our calculations show that pyrite RuO_2 is brittle under ambient conditions, while the brittleness decreases as pressure increases; the obtained results are shown in Fig.3. It is clear that the resistance to bond-length change greatly exceeds that to bond-angle change. Pettifor[52] suggested that the angular character of atomic bonding in metals and compounds, which could be related to the brittle or ductile properties of materials, could be described by the Cauchy pressure.

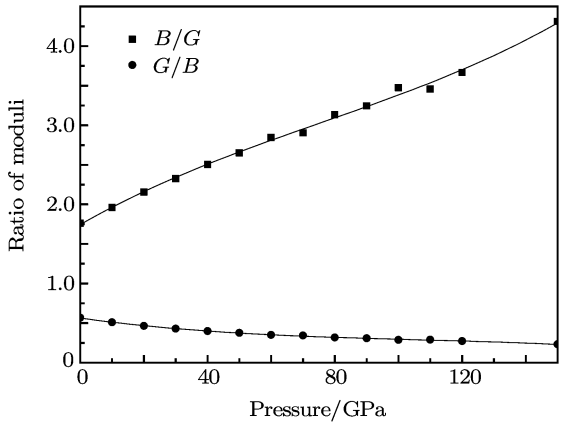


Fig.3. Ductility and brittleness as functions of pressure.

To learn something about the interatomic bonding, we use a Blackman diagram[47] plotted with the reduced c_{ij}. Figure 4 shows that RuO_2 falls on the low c_{44}/c_{11} side, away from covalent compounds which fall more in the centre.[47] This location suggests a strong ionic contribution and a weak covalent contribution. The Born instability conditions occur as lines c_{12}/c_{11}=1 and c_{44}/c_{11}=0, and the calculated points move toward the instability region.

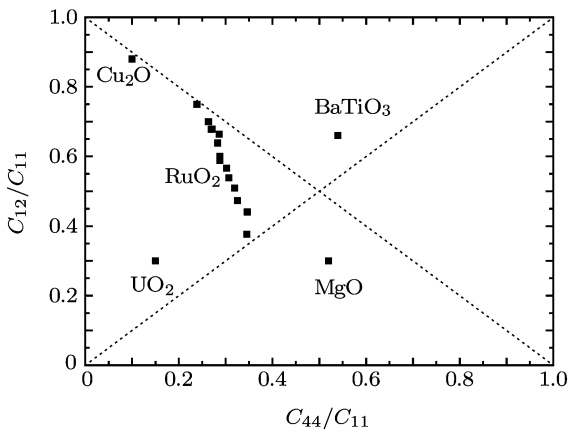


Fig.4. Blackman diagram showing points for RuO_2 and four other oxides.

Figure 5 shows that the heat capacity C_V is dependent on both the temperature T and the pressure P, which is due to the anharmonic approximation of the Debye model. The obtained heat capacity C_V versus a reduced temperature T/Θ indicates that heat capacity C_V reaches the Dulong–Petit limit with more difficulty under high pressures. It is obvious that the magnitude of the pressure dependence of C_V drops significantly at high temperatures, from –16.5% at room temperature to nearly zero at high temperature at 15% compression.

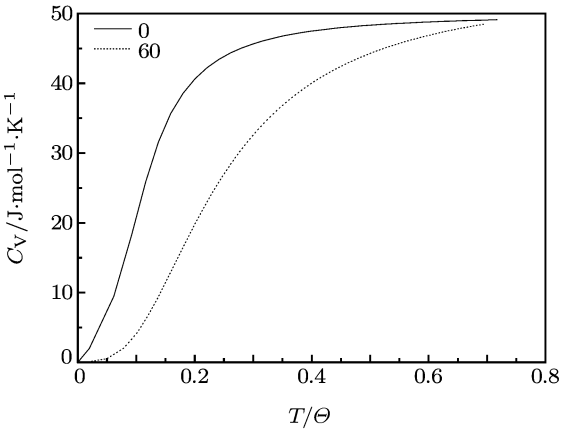


Fig.5. Heat capacity C_V as a function of the reduced temperature T/Θ under 0 and 60 GPa.

In Fig.6, the energy level shifts to higher energy in the conduction band and to lower energy in the valence band under pressure. The valence band maximum occurs at the axis of $M-G$ and the conduction band minimum occurs at the G point. A pseudogap appears

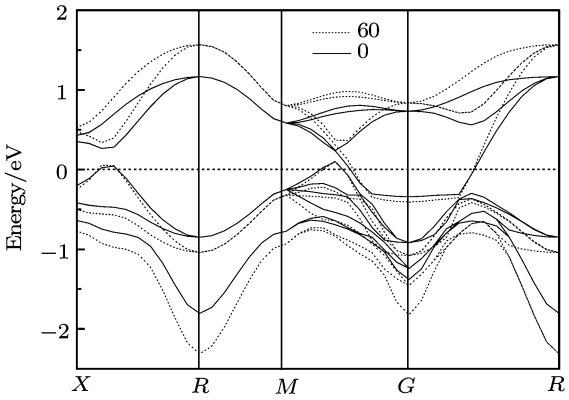


Fig.6. Energy band structure along the high symmetry points (X, R, M, G) in the Brillouin zone at pressures of 0 and 60 GPa. The Fermi level $E_{\rm F}$ is set to zero energy and is indicated by a horizontal dotted line.

between the bottom of the conduction band and the top of the valence band; unlike the cases of fluorite RuO_2,[3] the band structure shows strong metallic properties.

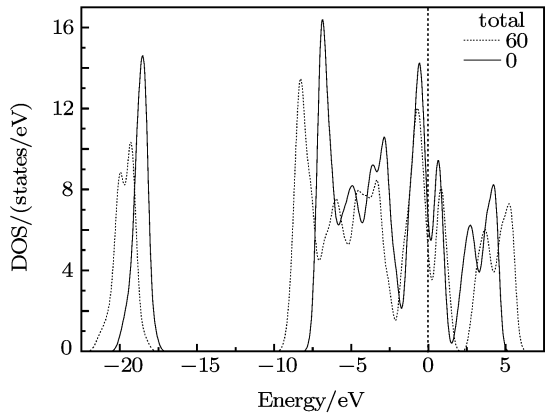


Fig.7. Total DOS correspondences to 0 and 60 GPa near the Fermi level E_F.

In Fig.7, the O 2s band is located at –18.5 eV, in good agreement with fluorite RuO_2.[17,18] The O 2s band width is about 4 eV; this result is larger than rutile RuO_2 with a width of 2.5 eV,[17] and is much larger than $CaCl_2$ RuO_2[17] with a width of 1.4 eV. In Fig.8(a), the minority O 2s density is located at 2.6 eV with an intensity of 0.05. The O 2p valence band width is 10.12 eV; this result is larger than rutile RuO_2 with a width of 5.9 eV or 6.8 eV,[18] and is also larger than that of fluorite RuO_2[17] with a width of 8.0 eV. The width of the O 2p conduction band in our calculation is about 6.74 eV, which is larger than fluorite RuO_2 with a width of 3 eV. At the Fermi level E_F, we have an overlap of the valence and conduction bands, revealing the metallic character. In the pyrite structure at E_F, the total density of state (DOS) contributed by O 2p density is 1.86, which is larger than the fluorite one (below 0.05),[18] the DOS contributed by Ru 4d (in Fig.9(a)) density is 4.6, which is also larger than the fluorite one (below 1.3), so the hybridization of Ru 4d and O 2p characters is more important in the pyrite structure than in the fluorite one. The bottom of the Ru 4d manifold is located at approximately –1.95 eV, which is slightly lower than fluorite RuO_2 with a value of –1.8 eV. However, the intensity of pyrite RuO_2 (0.65) is far larger than that of the fluorite phase (0.04). The main peak is located at –0.6 eV whereas it is –0.8 eV for the fluorite one, and the pyrite peak value is larger than fluorite RuO_2, having values of 11.55 and 3.05, respectively. Both results show a small shift in comparison with the rutile results[18] corresponding to –1.5 eV and –0.7 eV, respectively. The conduction bottom of the Ru 4d manifold is located at 1.5 eV with an intensity of 0.27. The fluorite RuO_2, however, is located at 0.36 eV with an intensity of 0.18. The E_F contributed predominantly by the O 2p and Ru 4d densities shows five sharp peak characters, unlike the rutile DOS[18] and fluorite RuO_2.[3]

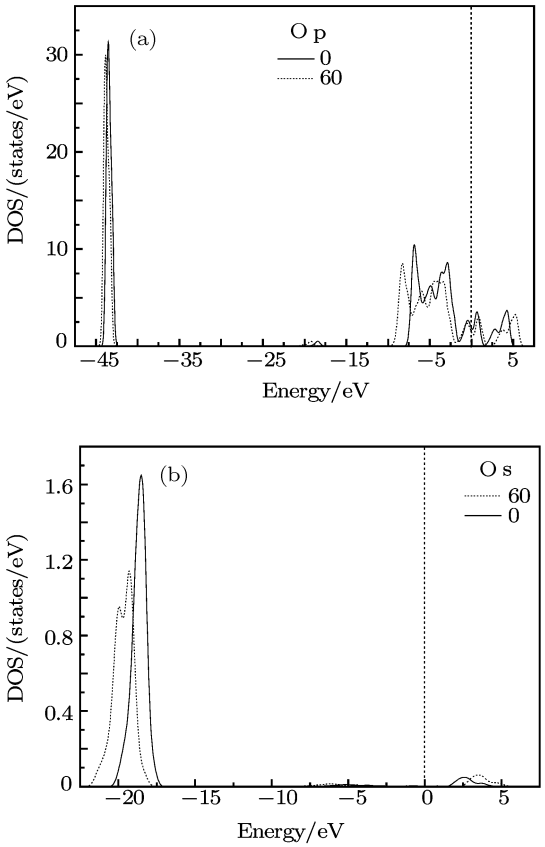


Fig.8. Partial DOS of O p state (a) and O s state (b) under 0 and 60 GPa.

To emphasize the pressure dependence of DOS, we calculated DOS under $P = 60$ GPa, together with $P = 0$ GPa plotted in Figs.8 and 9, from which we can see that pressure leads to a peak shift relative to E_F to higher or lower energies. Moreover, the intensity of DOS descends as pressure ascends. The change of DOS can be attributed to charge transfer during lattice distortion. With the increase of pressures, a higher overlap of the wave function results in a stronger delocalization of electrons. Electrons will transfer from the majority to minority spin band and form broader bands. The centre changes and electrons become more localized[53–55] when lattice distortion changes from negative to positive. The majority and minority bands will be moved relatively to E_F, which

will affect both the spin polarization ratio and magnetic properties. It is found that Ru 4d and O 2p states (including little O 2s states) overlap completely from –10 eV to 5 eV, which is evidently indicative of a covalent interaction between them resulting from strong hybridization.

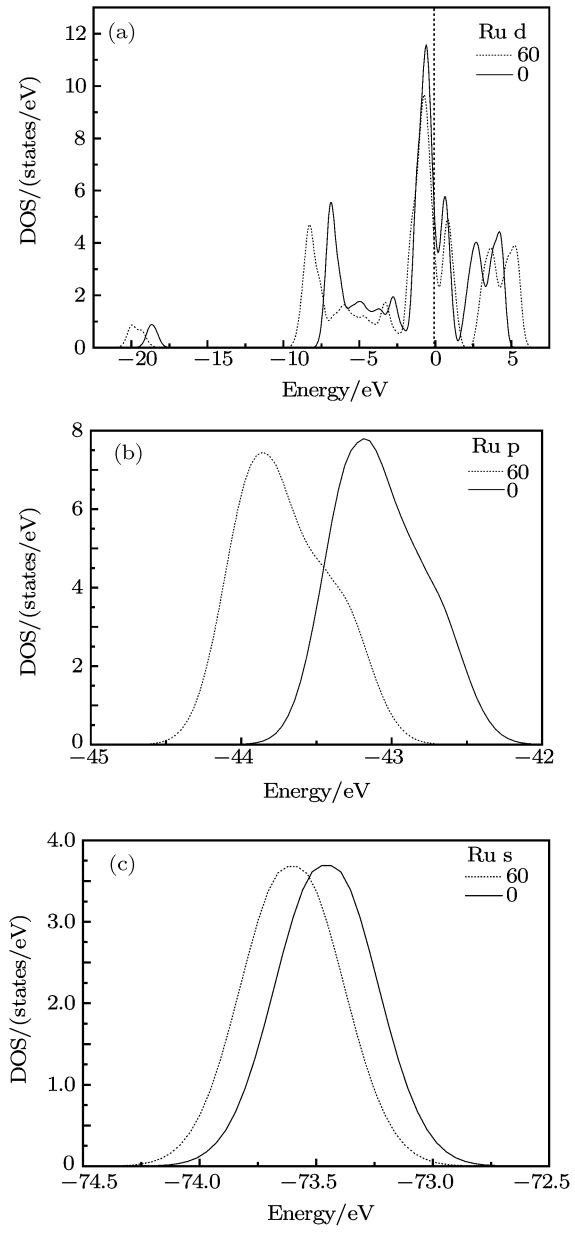


Fig.9. Partial DOS of Ru d state (a), Ru p state (b) and Ru s state (c) under 0 and 60 GPa.

The DOS of pyrite RuO_2 possesses a greater value (6.4) than fluorite RuO_2 (1.8) at the Fermi level, which indicates the strong metallic feature of pyrite RuO_2 in its crystalline state. The nearly free-electron states of the Ru are the principal reason for the metallicity of RuO_2.

In the pyrite structure, the low DOS at the Fermi level is responsible for the stabilization of the structure, where the pyrite level is higher than the fluorite phase, and the Fermi level falls in a sharp peak leading to a structural phase transformation induced by pressure. In Fig.7, the peak of total DOS at –0.56 eV is contributed mainly by Ru d states with a rather small contribution from O p states, and the total DOS at –0.56 eV below E_F arises mainly from the almost dispersionless bands along the $M-G$ and $G-R$ directions in the Brillouin zone. The lower [(–7.5)–(–2.5) eV] are dominated by the O p character but have a significant Ru d contribution to the bonding, while the unoccupied lying feature near E_F corresponds the antibonding part. The nearest E_F peak is formed mainly by the, to a first approximation, nonbonding Ru d_{eg} states.

Although there is a large hybridization between the Ru 4d and O 2p states, the charge transfer from Ru to O is nonnegligible in the present case. From the Mulliken population results, it is also found that charge transfer is as significant as about 1.02 electrons and shows insensitive pressure dependence. Therefore, the bonding behaviour between Ru–O has an ionic nature owing to charge transfer. Overall, the results show that the bonding nature in RuO_2 is a combination of covalent, ionic and metallic bonding, which contributes to the hardness and fundamental properties.

4. Conclusions

In summary, the obtained internal coordinate parameter increases with pressure. The elastic stability criteria show that the pyrite RuO_2 has elastic stability up to 150 GPa. For pyrite RuO_2, the Cauchy pressure is positive, while the fluorite RuO_2 has a negative pressure over a range of pressures from 0 to 115 GPa. The anisotropic parameter and normalized elastic constants of pyrite RuO_2 are elastically isotropic under ambient conditions. Heat capacity as a function of the reduced temperature shows that heat capacity depends on both the temperature and the pressure. A study of energy band structure presents a pseudogap at the Fermi level. The band structure, DOS, Poisson ratio, Blackman diagram and ductile–brittle relationship show that the bonding nature in RuO_2 is a combination of covalent, ionic and metallic bonding.

References

[1] Goodenough J B 1971 *Progress in Solid State Chemistry* (Vol.**5**) (Oxford: Pergamon Press)
Alder D 1968 *Solid State Physics* (Vol.**21**) (New York: Academic)

[2] Hugosson H W, Grechnev G E, Ahuja R, Helmersson U, Sa L and Eriksson O 2002 *Phys. Rev.* B **66** 174111

[3] Tse J S, Klug D D, Uehara K and Li Z Q 2000 *Phys. Rev.* B **61** 10029

[4] Trasatti S 1991 *Electrochim. Acta.* **36** 225

[5] Kawai T and Sakata T 1980 *Chem. Phys. Lett.* **77** 87

[6] Shafer M V and Armstrong J 1978 *IBM Tech. Discl. Bull.* **20** 4633

[7] Pedder J D 1976 *Science Technol.* (USA) **2** 259

[8] Leger J M and Haines J 1997 *Endeavour.* **27** 121

[9] Leger J M, Haines J and Blanzat B 1994 *J. Mater. Sci. Lett.* **13** 1688

[10] Haines J, Leger J M and Shulte O 1996 *Science* **271** 629

[11] Huntington J B 1958 *Solid State Physics* (Vol.**7**) (New York: Academic)

[12] Burdett J K 1985 *Inorg. Chem.* **24** 2244

[13] Haines J and Leger J M 1993 *Phys. Rev.* B **48** 13344

[14] Rosenblum S S, Weber W H and Chamberland B L 1997 *Phys. Rev.* B **56** 529

[15] Glassford K M and Chelikowsky J R 1993 *Phys. Rev.* B **47** 1732

[16] Lundin U, Fast L, Nordstrom L, Johansson B, Wills J M and Eriksson O 1998 *Phys. Rev.* B **57** 4979

[17] Benyahia K, Nabi Z, Tadjer A and Khalfi A 2003 *Physica* B **339** 1

[18] Yavorsky B Yu, Krasovska O V, Krasovskii E E, Yaresko A N and Antonov V N 1996 *Physica* B **225** 243

[19] Glassford K M and Chelikowsky J R 1994 *Phys. Rev.* B **49** 7107

[20] de Almeida J S and Ahuja R 2006 *Phys. Rev.* B **73** 165102

[21] Daniels R R and Margaritondo G 1984 *Phys. Rev.* B **29** 1813

[22] Leger J M, Djemia P, Ganot F, Haines J, Pereira A S and Jormada J A H 2001 *Appl. Phys. Lett.* **79** 2169

[23] Zhang H J, Lu B, Lu Y H, Huang H, Li H Y, Bao S N and He P M 2006 *Chin. Phys.* **15** 1892

[24] Payne M C, Teter M P, Allen D C, Arias T A and Joannopoulos J D 1992 *Rev. Mod. Phys.* **64** 1045

[25] Milman V, Winkler B, Packard C J, Payne M C, Akhmatskaya E V and Nobes R H 2000 *Int. J. Quantum. Chem.* **77** 895

[26] Vanderbilt D 1990 *Phys. Rev.* B **41** 7892

[27] Perdew J P, Burke K and Ernzerhof M 1996 *Phys. Rev. Lett.* **77** 3865

[28] Hammer B, Hansen L B and Norskov J K 1999 *Phys. Rev.* B **59** 7413

[29] Monkhorst H and Pack J 1976 *Phys. Rev.* B **13** 5188

[30] Murnaghan F D 1937 *Am. J. Math.* **59** 235

[31] Haines J, Leger J M, Schmidt M W, Petiter J P, Pereire A S, Jornada J A H and Hull S 1998 *J. Phys. Chem. Solids* **59** 239

[32] Sekkal W and Zaoui A 2001 *J. Phys.: Condens. Matter.* **13** 3699

[33] Swamy V and Muddle B C 2007 *Phys. Rev. Lett.* **98** 035502

[34] Zheng J C 2005 *Phys. Rev.* B **72** 052105

[35] Knittle E, Wentzcovich R M, Jeanloz R and Cohen M L 1989 *Nature* (London) **337** 349

[36] McSkimin H J and Bond W L 1957 *Phys. Rev.* **105** 116

[37] Alekasndrov I V, Goncharov A F, Zisman A N and Stishov S M 1987 *Soc. Phys. JETP* **66** 384

[38] Alekasndrov I V, Goncharov A F, Yakovenko E V and Stishov S M 1992 *High Pressure Research: Application to Earch and Planetary Sciences* (Washington, DC: American Geophysical Union) p409–416

[39] Wang J, Yip S, Philipot S R and Wolf D 1995 *Phys. Rev.* B **52** 12627

[40] Karki B B, Ackland G D and Crain J 1997 *J. Phys: Condens. Matter.* **9** 8579

[41] Chen C C, Wu Y J H and Wa L G 2000 *Mater. Chem. Phys.* **65** 306

[42] Tsuchiya T and Kawamura K 2002 *J. Chem. Phys.* **116** 2121

[43] Duffy T S, Shen G, Heinz D L, Shu J, Ma Y, Mao H K, Hemley R J and Singh A K 1999 *Phys. Rev.* B **60** 15063

[44] Chung D and Buessem W 1967 *J. Appl. Phys.* **38** 2010

[45] Francisco E, Blanco M A and Sanjurjo G 2001 *Phys. Rev.* B **63** 094107

[46] Haines J, Leger J M and Boequillon G 2001 *Annu. Rev. Matter. Res.* **31** 1

[47] Ledbetter H and Kim S 2001 *Handbook of Elastic Properties of Solids, Liquids and Gases* (Vol.II) (San Deigo: Academic Press) p281

[48] Voigt W 1928 *Lehrbuch der Kristallphysik* (Leipzig: Teubner) p716

[49] Reuss A 1929 *Z. Angew. Math. Mech.* **9** 49

[50] Hill R 1952 *Proc. Phys. Soc.* London Sect. A **65** 349

[51] Pugh S F 1954 *Phil. Mag.* **45** 833

[52] Pettifor D G 1992 *Mater. Sci. Technol.* **8** 345

[53] Block T, Carey M J, Gurney B A and Jepsen O 2004 *Phys. Rev.* B **70** 205114

[54] Kandpal H C, Fecher G H, Felesr C and Schonhense G 2006 *Phys. Rev.* B **73** 094422

[55] Luo H Z, Zhu Z Y, Li M, Xu S F, Wu G H, Liu H L, Qu J P and Li Y X 2008 *Physica* B **403** 605